

Electrochemistry of Vitamin B₁₂. I. Role of the Base-On/Base-Off Reaction in the Oxidoreduction Mechanism of the B_{12r}-B_{12s} System

D. Lexa^{1a} and J. M. Saveant^{*1b}

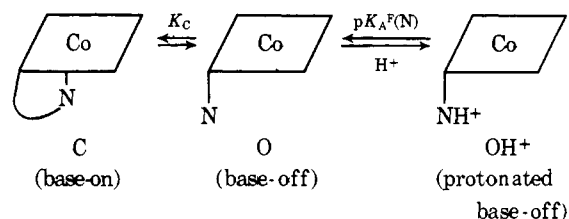
Contribution from the Laboratoire de Biophysique du Museum National d'Histoire Naturelle, 75 005 Paris, France, and the Laboratoire d'Electrochimie de l'Universit  de Paris VII, 75 221 Paris Cedex 05, France. Received July 1, 1975

Abstract: The mechanism of the electrochemical reduction of vitamin B_{12r} into B_{12s} is analyzed using mainly cyclic voltammetry. Adsorption of the neutral B_{12r} forms is minimized by addition of a solubilizing salt which allows a systematic investigation as a function of pH and sweep rate. The reduction mechanism involves, according to pH, the intermediacy of the protonated and neutral base-off B_{12r}, II-OH⁺ and II-O, the base-on B_{12r}, II-C, the protonated and neutral base-off B_{12s}, I-OH and I-O⁻, the base-on B_{12s}, I-C⁻, and the cobalt hydride, I-OH₂⁻. Below pH 2.9 the reduction is fast, with II-OH⁺ giving rise to a mixture of I-OH and I-OH₂⁺, the latter being formed predominantly below pH 1. Kinetic control by the base-on/base-off reaction appears above pH 2.9 and increases up to pH 4.7, reaching then a steady magnitude. The first reduction path then involves II-O continuously regenerated from II-C by the rate-determining coordination of the nucleotide side chain. Direct rate-determining electron transfer to II-C is observed at more negative potentials leading to I-C⁻ which is immediately converted into I-O⁻. Thermodynamic and kinetic data featuring quantitatively the oxidation-reduction process are given.

The cobalt atom in vitamin B₁₂ derivatives can exist in three different oxidation states ranging from III to I. Oxidation-reduction phenomena are thus of key importance in the chemistry of vitamin B₁₂.² The same is true of the enzymatic reactions of naturally occurring derivatives of vitamin B₁₂. For example, several redox couples have been shown to be involved in the methylcobalamin-dependent biogenesis of methane and acetic acid.^{3,4} Electrochemistry may therefore be considered as a valuable source of data for the chemistry and biochemistry of vitamin B₁₂. Indeed, several electrochemical studies have been devoted to the various vitamin B₁₂ derivatives. Most of them were polarographic and concerned mainly the cyano and aquocobalamins.⁵⁻¹¹ However, the deoxyadenosyl, methyl, and other alkylcobalamins¹²⁻¹⁵ and cobinamides,^{13,14} the hydroxo-¹³ and sulfitecobalamins^{14,15} and vitamin B_{12s}¹⁶ have also been studied. More recently, cyclic voltammetry (CV) has been employed to characterize the electrochemical behavior of B₁₂,^{17,18} B_{12a},^{18,19} B_{12r},^{17,19} B_{12s},¹⁷ and of methyl and trifluoromethylcobalamins¹⁸ and of methyl and B_{12r} cobinamides.¹⁸ Controlled potential electrolysis and coulometry have also been used to prepare and characterize the reduced states of cyano- and aquocobalamin.^{16,20-22} Potentiometry has been much less employed; only two studies have appeared which were concerned with the measurement of the B_{12r}-B_{12s} standard potential.^{19,23}

Most of this electrochemical work was aiming at the determination of equilibrium parameters, namely, the standard potentials of the successive redox couples in connection with changes in axial coordination. Except for a few reversibility estimations,¹⁷⁻¹⁹ no analysis of the kinetics of the electron-transfer processes and of the related ligand-transfer reactions has apparently been attempted. This seems to be largely because of the occurrence of reactant adsorption which complicates the overall electrochemical behavior since it contributes, together with diffusion, to the observed currents and it may inhibit the electrochemical reaction itself. The consequence is not only a paucity of kinetic data but also the difficulty of deriving meaningful thermodynamic equilibrium potentials from the polarographic and CV curves which results in poor agreement between the various determinations (see, e.g., ref 19).

The present work attempts to provide a more detailed analysis of the kinetics of the B_{12r}-B_{12s} couple with particular emphasis on the role of the cobalt coordination by the 5,6-dimethylbenzimidazole located at the end of the nucleotide side chain (Bzm). In this connection the effect of pH has been systematically investigated. pH is indeed an operational parameter for varying the relative amounts of the base-off and base-on species at equilibrium according to the following scheme, which applies to the three oxidation states.



The equilibrium thermodynamics of the system can be characterized by two independent parameters, e.g., the chain-closing constant, $K_C = a_C/a_O$, and the pK_A of the cobalt free Bzm, $pK_A^F(\text{N})$. The acid-base titration of the system would lead to a pK_A , $pK_A(\text{N})$, corresponding to

$$K_A(\text{N}) = [(a_C + a_O)/a_{\text{OH}^+}]a_{\text{H}^+}$$

which reflects the competition between protonation and cobalt coordination of the Bzm nitrogen atom. The three constants are related by the following equation.²

$$pK_A(\text{N}) = pK_A^F(\text{N}) - \log(1 + K_C) \quad (1)$$

$pK_A^F(\text{N})$ can be considered with a good approximation as being equal to the pK_A of the free Bzm nucleotide, 4.7, so that measuring $pK_A(\text{N})$ leads immediately to a value of K_C . These determinations have so far been performed mainly in the case of Co^{III} cobalamins as a function of the sixth axial ligand.² For Co^{II} an approximate determination by ESR spectroscopy led to $pK_A^{\text{II}}(\text{N}) = 2.5$.²⁴ For B_{12s}, as far as the cobalt is not involved in a hydridic structure, it can be assumed that coordination of the Bzm is virtually absent leading to $pK_A^{\text{I}}(\text{N}) \approx 4.7$. However, possible protonation of the cobalt atom itself must be taken into account result-

ing in an hydridocobalamin in which Bzm coordination cannot a priori be excluded.

The reduction mechanism of B_{12r} into B_{12s} will be described within this thermodynamic framework leading to the determination of a series of kinetic and equilibrium parameters. Among the latter, the determination of the Bronsted basicity of B_{12s} has been described in detail elsewhere.²⁵

Experimental Section

Chemicals. Vitamin B_{12a} was obtained from Roussel-Uclaf. Its purity was checked by column chromatography on cationic cellulose²⁶ and controlled by absorption spectrometry.²

The solutions were prepared either from perchloric acid in concentrations ranging from 1.2 to 0.1 M or from Britton-Robinson buffers obtained by addition of sodium hydroxide to a mixture of acetic, boric, and phosphoric acids.²⁷

Tetrabutylammonium *p*-toluenesulfonate (TBATS) was prepared by neutralization of an aqueous solution of tetrabutylammonium hydroxide by *p*-toluenesulfonic acid (Prolabo products) so as to obtain a 1.6 M final concentration.

Cell and Electrodes. Cyclic voltammetry and controlled potential electrolysis (CPE) were performed in inactinic cells containing 1–2 mM solutions. The temperature was 22 °C. The solutions were deaerated by bubbling argon and were maintained under argon during the experiment. For the alkalimetric determination of $pK_A^{11}(N)$ the cell was placed in a glove box flushed with argon.

A three electrode system was used comprising a mercury pool or a platinum anode and a saturated calomel reference electrode separated from the cell by a bridge containing the same supporting electrolyte. All potentials are referred to the SCE. A platinum gauze electrode was used as a cathode in the CPE experiments. In CV two kinds of working electrodes were employed: for sweep rates above 0.1 $V s^{-1}$ a knock-off dropping mercury electrode (DME) with a delay time of 25 s; for lower sweep rates a stationary mercury drop hanging from a gold disk (HME).

Instrumentation. The CV apparatus was composed of a function generator (Tacussel GSTP3) and a solid-state potentiostat implemented with a positive feedback ir drop compensation.²⁸ The latter device was found useful with most of the solutions, the resistance uncompensated by the potentiostat itself being on the order of several hundred ohms. When a dropping mercury electrode was used, the function generator was synchronized with the drop dislodgement so that the triangular sweep was applied at the end of the drop life. The electrode surface area could thus be considered as practically constant during the potential sweep. The current-potential curves were displayed on a storage oscilloscope (Tektronix 7313). The peak potentials were determined by placing the spot on the peak by means of the dc voltage source of the generator and reading the result on a digital voltmeter.

For CPE, a 2A-20V potentiostat (Tacussel PRT) was used together with a coulometer (Tacussel I65).

Results

Most of the CV experiments were performed on a B_{12a} solution with the initial potential of the sweep in the range –0.4 to –0.6 V where B_{12a} is reduced into B_{12r} . The duration of this in situ preelectrolysis was 25 s with the DME and even longer with the HME. It can be assumed that under such conditions the results are the same as if B_{12r} would have been the actual starting material. This point was established for one pH (5) and assumed to hold for the others. It was checked that the curves thus obtained at pH 5 starting from B_{12a} are the same as those recorded after exhaustive electrolysis of B_{12a} at –0.35 V on platinum.

The present study is restricted to pH below 8 since at higher pH's B_{12r} exhibits a tendency toward disproportionation. It is observed accordingly that the CV Co^{III}/Co^{II} and Co^{II}/Co^I wave systems begin to merge in this pH range. The analysis of the disproportionation process and of the B_{12a} reduction in alkaline media will be the subject of a forthcoming publication.

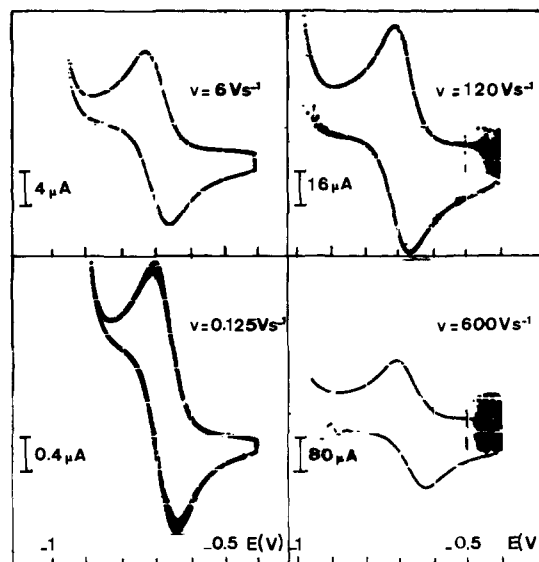


Figure 1. CV curves in 0.3 M $HClO_4$ as a function of sweep rate: B_{12} concentration, 2 mM; electrode, DME.

In acidic media, i.e., below pH 2 the i - E patterns appear as perfectly reversible, showing neither detectable adsorption of reactants nor any influence of associated chemical reactions. An example of this behavior is given in Figure 1 in the case of a 0.3 M perchloric acid solution. Up to 120 $V s^{-1}$ the peak potential separation is close to the theoretical value, 56 mV, representative of a Nernstian diffusion controlled system.^{29,30} The increase of the peak separation observed on further raising the sweep rate (see Figure 1) may be attributed to the effect of the residual resistance remaining after positive feedback compensation.²⁸ It follows that the kinetics of the charge-transfer process does not seem to interfere within the considered sweep rate range.

In the most acidic medium considered in this work, 1.2 M $HClO_4$, some departure from reversibility is observed at low sweep rate (see Figure 1, A, in ref 25). The cathodic wave tends to become S-shaped and the anodic trace to be closer and closer to the cathodic one. At the same time the peak, or plateau, current is larger than predicted by the i - $V^{1/2}$ proportionality observed at higher sweep rates.

In these acidic media it is also apparent that the proton discharge current-potential curve is shifted toward more positive potentials when B_{12a} is present in the solution. The shift depends upon the sweep rate and is of the order of 100 mV.

A different type of departure from reversibility appears progressively on raising the pH above 3. Two typical examples selected in a series of experiments at pH's ranging from 3 to 7 are given in Figure 2 which shows the curves obtained at pH 4 and 7 for various sweep rates. Two cathodic waves and still one anodic wave are now observed. The magnitude of the second cathodic wave increases relative to the first wave with the sweep rate. The same ratio also increases with pH at low sweep rate. Concomitantly, the first peak flattens, resulting in an S-shaped wave.

It is, however, apparent that the i - E curves are distorted by adsorption of the reactants, being increasingly drawn out along the E axis as the sweep rate is raised. These effects, that may be ascribed to self-inhibition of the oxidation-reduction processes, are more and more pronounced on raising the pH between 3 and 5 and remain of the same order of magnitude above pH 5. At pH 7, for example, three ill-defined waves appear at 33 $V s^{-1}$ (Figure 2).

The interference of reactant adsorption greatly complicates the analysis of the CV curves, thus hampering an ac-

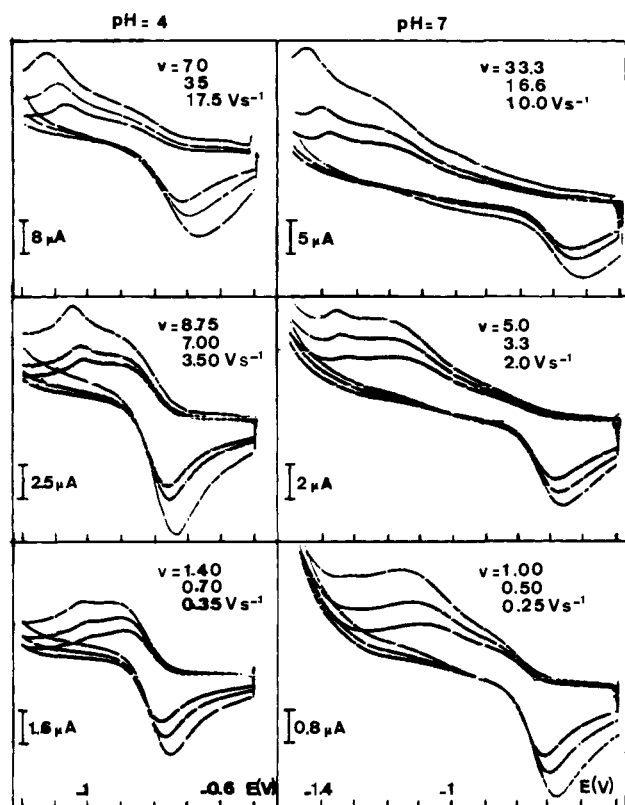


Figure 2. CV curves at pH 4 and 7 as a function of sweep rate: Britton-Robinson buffers; B_{12} concentration, 2.1 mM; electrode, DME.

curate determination of the oxidation-reduction mechanism. From the observation that the effect of adsorption becomes apparent above pH 3, it can be inferred that the adsorbed species are the base-on and unprotonated base-off B_{12r} and possibly unprotonated B_{12s} . Assuming poor solubility in water rather than strong chemical interaction with the mercury of the electrode to be responsible for adsorption in the present case, it may be expected that its influence will be decreased by addition of a water-soluble organic compound. The requirement of water solubility is best met by an organic salt. Then specific adsorption of the cation is expected to be a further factor favoring the desorption of the B_{12} species. Tetrabutylammonium *p*-toluenesulfonate (TBATS) was chosen for this purpose. Figures 3 and 4 show the effect of progressive addition of TBATS on the CV curves at 0.9 V s^{-1} for pH 4 and 7. At pH 4 a quasi-reversible adsorption wave of the Brdicka type^{31,32} appears near the supporting electrolyte discharge featuring a decrease in self-inhibition. It shifts toward positive potentials when raising the TBATS concentration. It then merges with the diffusion wave and finally disappears, leading to an apparently adsorption-free CV pattern. At pH 7 the Brdicka peaks first appear closer to the diffusion waves, then move negatively upon further TBATS addition, and finally disappear. It is seen that more TBATS is required to eliminate adsorption at pH 7 than at pH 4.

It was noted, moreover, that once the effect of adsorption has been suppressed at a given sweep rate it may reappear for faster sweeps. This is even more apparent when sweeping in the reverse direction from a potential where B_{12s} is the starting species. A typical example of this is given in Figure 5 for pH 7 at 12 V s^{-1} .

It is seen that for 1.45 mM B_{12s} solutions a concentration of 0.44 M TBATS is necessary to suppress the adsorption effect at this sweep rate. On raising the sweep rate, the adsorption peak reappears and more TBATS is required for

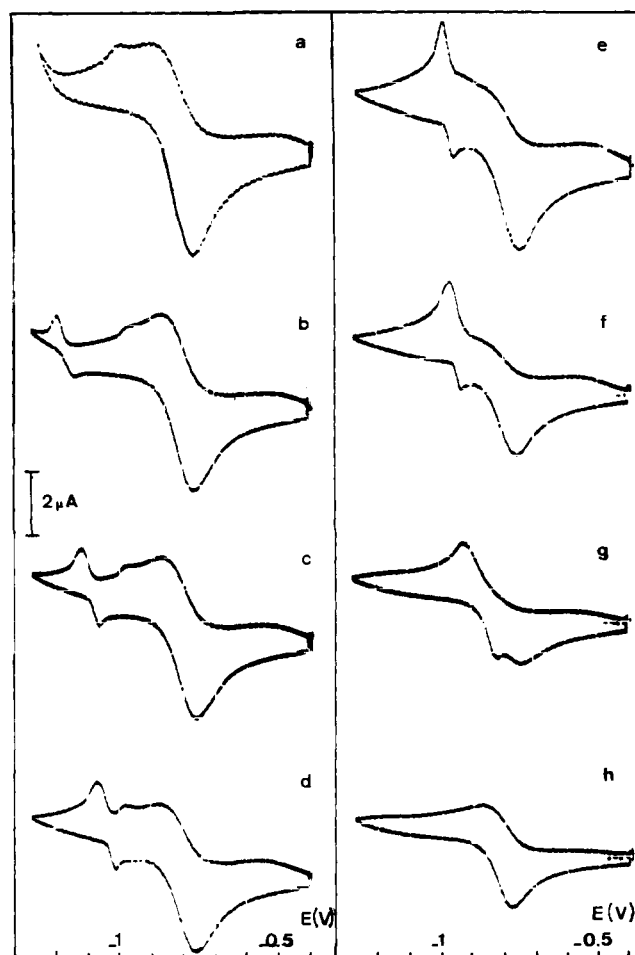


Figure 3. CV curves at pH 4 as a function of TBATS addition: sweep rate, 0.9 V s^{-1} ; electrode, DME; TBATS concentration (M), (a) 0.00, (b) 0.03, (c) 0.06, (d) 0.09, (e) 0.12, (f) 0.15, (g) 0.27, (h) 0.33; B_{12} concentration (mM), (a) 2.00, (b) 1.96; (c) 1.92, (d) 1.89, (e) 1.85, (f) 1.82, (g) 1.67, (h) 1.59.

its elimination. It was noticed that elimination of adsorption according to this more stringent procedure requires more and more TBATS from pH 3 to 5 and approximately the same amount above pH 5. In order to get rid of the influence of adsorption up to 1000 V s^{-1} , in the whole pH range for a B_{12} concentration of 1.11 mM, a concentration of 0.72 M TBATS was found necessary. Further additions did not result in any noticeable change on the direct and reverse CV traces at rates of 1000 V s^{-1} and below. These conditions were therefore used above pH 3 for the analysis of the oxidation-reduction mechanism from the variations of the CV curves with sweep rate. It was noticed that introduction of TBATS also has the effect of increasing the pH as measured with a conventional glass electrode. Addition of 4 ml of a 1.6 M solution to the initial 5-ml solution leading to a 0.72 M TBATS concentration results in an approximately constant increase of about 0.8 pH units in the considered pH range.

The CV curves were studied with these conditions as a function of the sweep rate v at several pH's ranging from 3 to 8. Three examples of the observed behaviors are shown in Figures 6-8 corresponding respectively to pH 4.2, 5.8, and 7.9.

The essential features displayed by the voltammograms represented on the figures and those obtained at other pH's in the same range are the following. (i) Two cathodic and one anodic waves are observed for most sweep rates. (ii) The second wave tends to disappear at low sweep rate and a

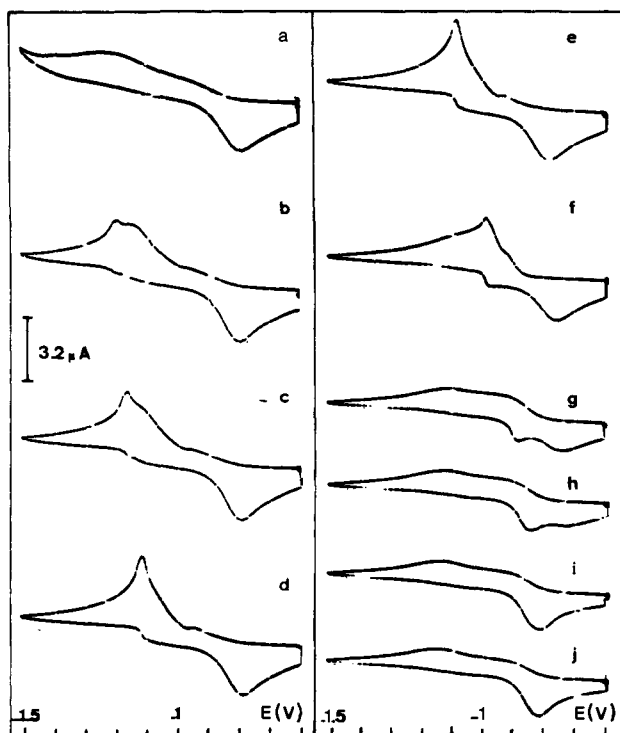


Figure 4. CV curves at pH 7 as a function of TBATS addition: sweep rate, 0.9 V s^{-1} ; electrode, DME; TBATS concentration (M), (a) 0.00, (b) 0.02, (c) 0.03, (d) 0.06, (e) 0.12, (f) 0.22, (g) 0.31, (h) 0.35, (i) 0.39, (j) 0.42; B_{12} concentration (mM), (a) 2.08, (b) 2.06, (c) 2.04, (d) 2.00, (e) 1.93, (f) 1.79, (g) 1.68, (h) 1.62, (i) 1.58, (j) 1.53.

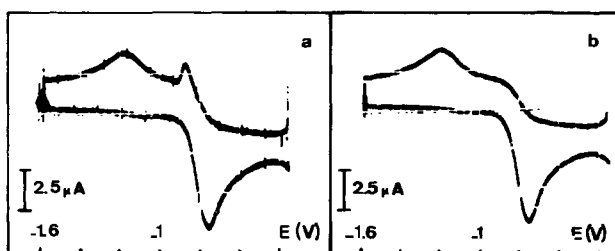


Figure 5. Reverse CV curves at pH 7; sweep rate, 12 V s^{-1} ; TBATS concentration, (a) 0.41 M, (b) 0.44 M; B_{12} concentration, (a) 1.45 mM, (b) 1.49 mM.

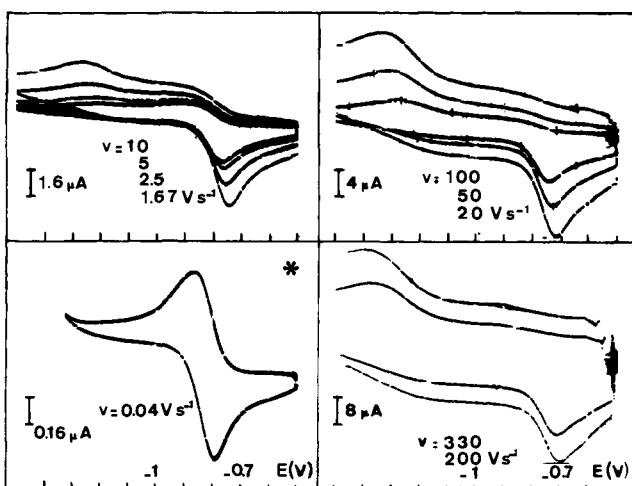


Figure 6. CV curves at pH 4.2 as a function of sweep rate: TBATS concentration, 0.71 M; B_{12} concentration, 1.15 mM; electrode, DME; *, HDME.

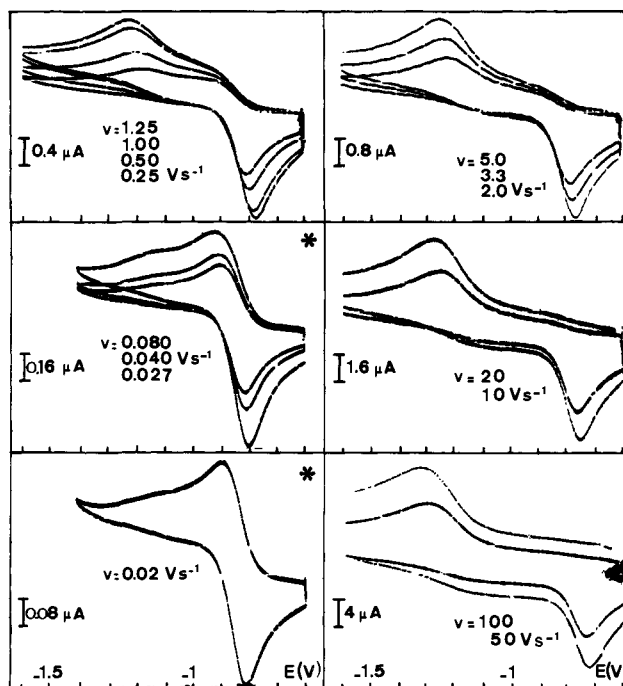


Figure 7. CV curves at pH 5.8 as a function of sweep rate: TBATS concentration, 0.71 M; B_{12} concentration, 1.2 mM; electrode, DME; *, HDME.

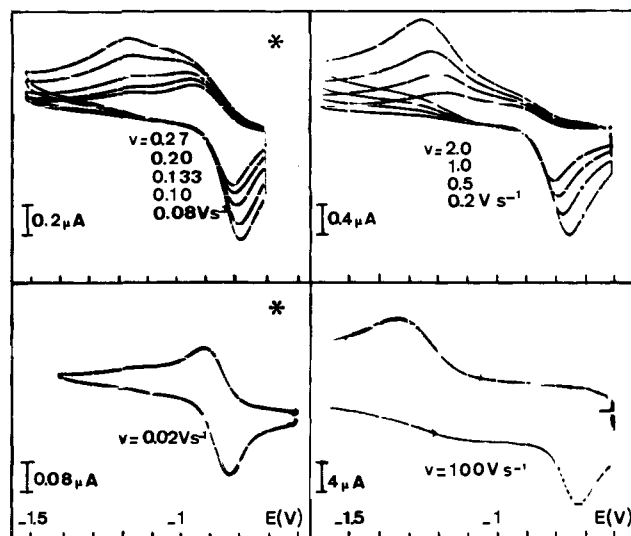
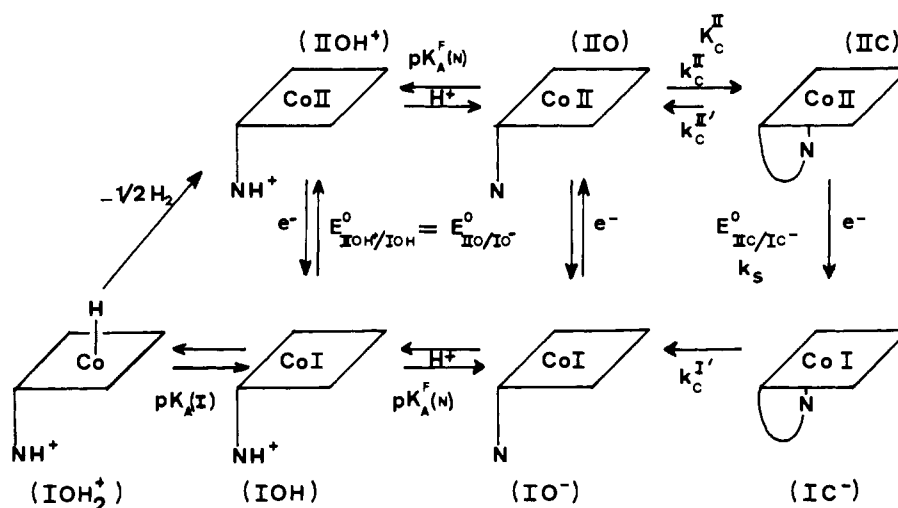


Figure 8. CV curves at pH 7.9 as a function of sweep rate: TBATS concentration, 0.71 M; B_{12} concentration, 1.1 mM; electrode, DME; *, HDME.

nearly reversible pattern is then obtained. (iii) The first cathodic peak flattens as v increases and takes the form of an S-shaped wave, the height of the plateau-current increasing then slowly with v , i.e., markedly less than $v^{1/2}$. (iv) The height of the second cathodic peak increases more rapidly than $v^{1/2}$ so that the first wave becomes negligible compared with the second one at high sweep rates. (v) As v increases the anodic peak distinctly shifts toward more positive potentials, the second cathodic peak toward negative potentials, and the first cathodic wave slightly shifts toward positive potentials. When v is such that the first cathodic wave is small the anodic peak shifts by about 30 mV per decade and the peak-width is close to 50 mV. At the same time the second cathodic peak shifts by 60–70 mV per decade and the peak width is 100–110 mV. (vi) The various features of the dependence of the CV curves upon the sweep

Scheme I



rate remain approximately the same above pH 5. (vii) Below pH 5, the wave system is more and more reversible as the pH decreases and the magnitude of the first wave relative to the second one becomes larger and larger at a given sweep rate. (viii) Up to about pH 5 the background discharge is again shifted positively. Above this pH, the observed behavior becomes more complex due probably to the interference of Na^+ discharge. This phenomenon needs further investigation.

Discussion

The general aspect of the CV curves above pH 3 and their variation with the sweep rate is typical of a reduction process involving a homogeneous chemical reaction preceding the electron-transfer step.^{33,34} Owing to electron donation by the Bzm ligand the base-on form of B_{12r} , II-C, is obviously less easily reduced than the base-off forms, II-O and II-OH⁺. The first cathodic wave may therefore be attributed to the reduction of the base-off forms and the second one to that of the base-on form (Scheme I).

When the solution is made more and more acidic the proportion of the base-off components, in the form of II-OH⁺, increases at the expense of the base-on form. The kinetic control by the coordination reaction diminishes accordingly and the system tends to become reversible as observed experimentally. Conversely, when raising the pH the relative proportion of base-on and base-off (under the form of II-O) species tends toward a limit and so does the kinetic character of the first cathodic wave in agreement with the experimental observations.

The oxidation-reduction mechanism of the B_{12r} - B_{12s} couple may therefore be depicted by the above scheme, the relative role of each species depending on the pH.

No kinetic influence of the protonation reactions either at the Bzm nitrogen in the Co^{II} and Co^{I} base-off species or at the cobalt atom in B_{12s} is apparent in the considered pH range even at very high sweep rate. II-OH⁺ and II-O on one hand and I-OH₂⁺, I-OH, and I-O⁻ on the other may therefore be considered at equilibrium whatever the sweep rate and the pH. The contribution of II-OH⁺ to the first cathodic kinetic wave thus decreases when the pH is raised in favor of II-O. The observed shift of the anodic peak by 30 mV per decade when the system has reached its highest irreversibility is in agreement with a fast reoxidation of the B_{12s} base-off forms resulting first in a base-off B_{12r} followed by a rate-determining conversion into the base-on form.^{35,36}

The second cathodic wave corresponds to the direct reduction of the base-on B_{12r} leading to a base-on B_{12s} , I-C⁻,

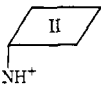
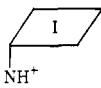
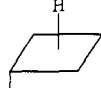
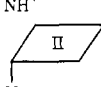
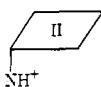
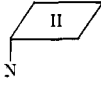
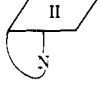
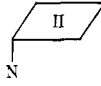
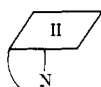
which is expected to be extremely unstable due to the fact that Co^{I} is certainly a very poor electrophile. The electron transfer is thus followed by the fast conversion of the base-on B_{12s} into its base-off forms. This is in agreement with the shifting of the second cathodic peak with the sweep rate. The magnitude of the shift rate and that of the peak width indicates that the rate-determining step is here the electron transfer itself and not the succeeding deligandation reaction which would lead to a 30-mV shift and a 50-mV width.^{29,36} This is most probably related to the high rate of the deligandation reaction rather than to an intrinsic slowness of the electron transfer.³⁶

Finally, the features of the CV curve in very acidic medium are consistent with a slow decomposition of the hydric species evolving hydrogen and regenerating B_{12r} ,^{16,22,37,38} hence giving rise to a catalytic wave³⁹⁻⁴¹ at slow sweep rates. The positive shift of the background discharge may be attributed to the reduction of the cobalt hydride I-OH₂⁺ which gives rise to a much more efficient catalytic H⁺ discharge. At higher pH a similar process may occur even though the equilibrium concentration of I-OH₂⁺ becomes small. It cannot, however, be excluded that a base-on cobalt hydride might be formed through protonation of the initial reduction product of II-C, I-C⁻, which is expected to be markedly more basic than I-OH and that this CoH compound would relay I-OH₂⁺ as a catalyst for the hydrogen discharge. This problem clearly needs further investigation.

The standard potential E^0 featuring the conversion of II-C + II-O + II-OH⁺ into I-O⁻ + I-OH + I-OH₂⁺ can be readily derived from the reversible CV curves which are obtained in a large range of sweep rates below pH 3 and at low sweep rate above pH 3. The variation of E^0 with the pH is shown in Figure 9.

The diagram is composed of two horizontal and two oblique segments whose slope is close to 60 mV/pH unit. The pH values featuring the transition between them are successively 1, 2.9, and 4.7. The second value is close to the approximate result previously obtained for $\text{pK}_A^{\text{II}(\text{N})}$.²⁴ We have verified by acid-base titration under an argon atmosphere of a solution of B_{12r} prepared by exhaustive electrolysis of B_{12a} on platinum that 2.9 is indeed the correct value for this pK_A . The third value is the same within experimental error as the pK_A of the free Bzm² and may be taken as equal to the pK_A of the II-OH⁺/II-O and I-OH/I-O⁻ couples. It is noted that considering the pK_A of uncoordinated Bzm as the same in II-O and I-O⁻ implies that the standard potentials $E^0_{\text{II-OH}^+/\text{I-OH}}$ and $E^0_{\text{II-O}/\text{I-O}^-}$ are also equal. As discussed previously²⁵ the first pK_A is that of the couple I-

Table I. Thermodynamic and Kinetic Constants of $B_{12r}-B_{12s}$ Oxidoreduction

pK _A and Equilibrium Constants	
	$pK_{A}^{II(N)} = 2.9$
	$pK_{A}^{I(N)} = 4.7$
	$pK_{A}^{(I)} = 1$
	$k_C = 62$
Standard Potentials	
	$E^0_{II-OH^+/I-OH} = -0.740 \text{ V vs. SCE}$
	$E^0_{II-O/I-O^-} = -0.742 \text{ V vs. SCE}$
	$E^0_{II-C/I-O^-} = -0.851 \text{ V vs. SCE}$
Chemical Rate Constants	
	$k_C^{II} = 10^5 \text{ s}^{-1}$ $k_C^{II'} = 1.6 \times 10^3 \text{ s}^{-1}$
Electron-Transfer Kinetics	
	$k_S \exp[(\alpha F/RT)E^0_{II-C/I-C^-}] = 2.5 \times 10^{-12} \text{ cm s}^{-1}$ ($\alpha = 0.45-0.5$)

$\text{OH}_2^+/I\text{-OH}$ which features the Bronsted basicity of the cobalt in base-off B_{12s} . The zones of thermodynamic stability of the various Co^{II} and Co^I species can be assigned as shown in Figure 9. The various thermodynamical constants that can be derived from the E^0 -pH plot are given in Table I.

The value of K_C was derived from $pK_{A}^{II(N)}$ and $pK_{A}^F(N)$ using eq 1. as expected the values obtained for $E^0_{II-OH^+/I-OH}$ and $E^0_{II-O/I-O^-}$ are the same within experimental error. The value found for $E^0_{II-O/I-O^-}$, -0.85 V , which features the equilibrium conversion of B_{12r} to B_{12s} above pH 4.7 is not far from the previous potentiometric determinations (-0.86 and -0.83 V)^{19,23} but differs more significantly from those obtained polarographically which range between -0.88 and -1.07 V .^{8,13,17,19} On the contrary, the value found for $E^0_{II-OH^+/I-OH}$ (-0.74 V) agrees well with a previous polarographic determination at pH 2.4 and 2.8.^{13,19} This is to be related to the effect of adsorption which was not eliminated in the previous polarographic determinations and therefore is likely to have been interfering above pH 5 and not below this pH as shown above. Among the reactions shown on the mechanism chart thermodynamic data featuring the $II-C-I-C^- - I-O^-$ sequence are not obtainable through the present analysis due to the very large chemical instability of the base-on B_{12s} .

The analysis of the kinetic influence of the B_{12r} base-off/base-on reaction on the electrochemical reduction is simplified by the assumption that the Co^{II} and Co^I base-off forms remain at equilibrium. Under these conditions the kinetic

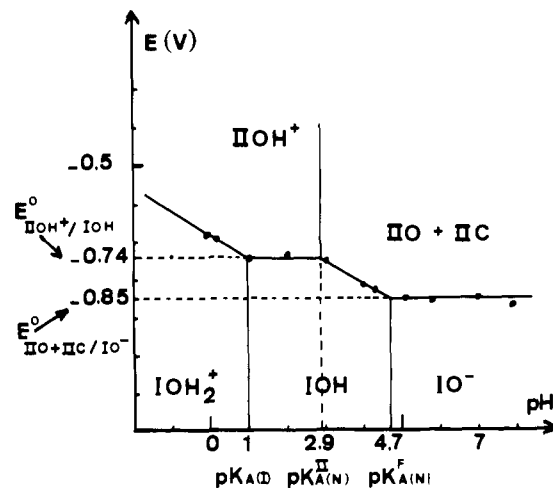
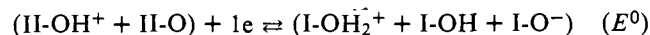
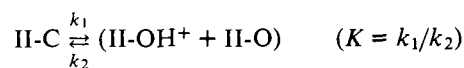


Figure 9. Standard potential vs. pH plot.

character of the first cathodic wave can be considered the result of the influence of the chemical reaction in the following reaction scheme



with $k_1 = k_C^{II'}$, $k_2 = k_C^{II}/(1 + 10^{4.7-pH})$, $K = 10^{-1.8} + 10^{2.9-pH}$, and E^0 being given as a function of pH by the diagram in Figure 9. One can then resort to the results of the formal kinetic analysis of systems involving a single antecedent chemical reaction,^{33,34} particularly as regards the determination of the chemical rate constants. An approximate evaluation of these constants was made using the working curves of Figure 5 in ref 33 which give for each K the value of $i_p^c/0.446FSC^0D^{1/2}(Fv/RT)^{1/2}$ as a function of $\log [RT(k_1 + k_2)/Fv]$ (where i_p^c is the plateau or peak current of the first cathodic wave, S the electrode surface area, C^0 the initial concentration, and D the value of the diffusion coefficients of the various species which are assumed to be equal). The evaluation was performed at pH 5.8 for $v = 0.50, 1.00, 1.25, 2.00, 3.33,$ and 5.00 V s^{-1} , at pH 7.9 for $v = 0.50, 1.00,$ and 2.00 V s^{-1} , and at pH 4.2 for $v = 5.00$ and 10.00 V s^{-1} . The value of the denominator of the dimensionless current function was derived from the height of the anodic peak which tends approximately toward $0.496FSC^0D^{1/2}(Fv/RT)^{1/2}$ at sufficiently high sweep rate. Under these conditions a fairly constant value of 10^5 s^{-1} was found for $k_1 + k_2$ which leads to $k_C^{II} = 10^5 \text{ s}^{-1}$ and $k_C^{II'} = 1.6 \times 10^3 \text{ s}^{-1}$.

The variations of $\log K$ and $\log (k_1 + k_2)$ with pH are shown in Figure 10a,b. Using these plots and the kinetic zone diagram previously established,³³ Figure 10c shows how the system becomes kinetically controlled by the chemical reaction in the range $0.02-100 \text{ V s}^{-1}$ as the pH varies. It is seen in agreement with experiment that (i) a nearly reversible behavior is obtained at the lowest sweep rate whatever the pH, (ii) as the pH decreases the kinetic character at a given sweep rate decreases and reversibility is more and more easily reached, and (iii) above pH 5 the kinetic character of the system remains the same.

As regards the kinetics of the rate-determining electron transfer to base-on B_{12r} , the peak shift with sweep rate and the peak width indicate a value of the transfer coefficient α on the order of 0.45-0.50. The forward rate constant as determined²⁹ from the position of the peak is

$$k_S \exp[(\alpha F/RT)E^0_{II-C/I-C^-}] = 2.5 \times 10^{-12} \text{ cm s}^{-1}$$

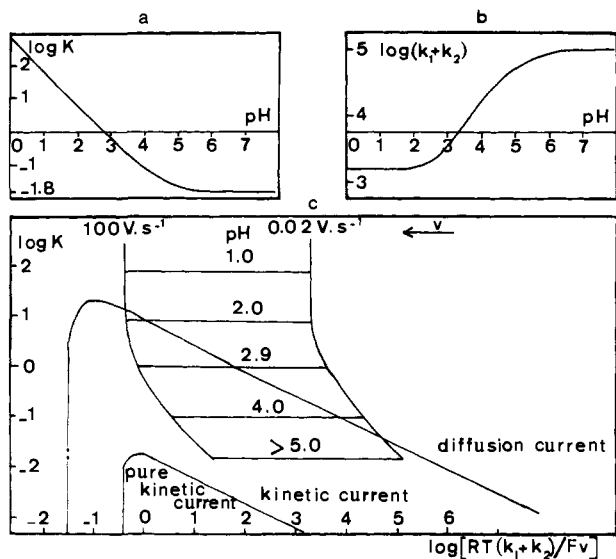


Figure 10. Sketch of the kinetic control of the B_{12r} - B_{12s} system by the base-off/base-on reaction according to pH.

where k_S is the exchange rate of the electron transfer. The diffusion coefficient was estimated as $3 \times 10^{-6} \text{ cm}^2 \text{ s}^{-1}$ from previous determinations¹³ corrected for the effect of TBATS which was itself obtained from the ratio of the peak currents with and without TBATS. Only the forward rate and not the exchange rate can be derived from the CV curves due to the fast and irreversible decomposition of $I-C^-$ which hampers the determination of $E^0_{II-C/I-C^-}$.

The present study allows some general conclusions to be drawn that may be of significance in the analysis of chemical and biochemical oxidation-reduction processes involving the B_{12r} - B_{12s} couple. B_{12r} may be reduced according to two different reaction paths. The first one involves the reduction of the base-off forms where the rate-determining reaction above pH 2.9 is then the decoordination of the cobalt atom from the nucleotide side chain. The second one, which occurs at more negative potentials, involves the reduction of the base-on form with the electron transfer then being the rate-determining step. If a relatively low flux of electrons is required in the reduction process, the electron transfer involves base-off B_{12r} at all pH values. For a higher flux of electrons the major route tends, as the pH increases, to involve a direct electron transfer to the base-on B_{12r} which necessitates a stronger reducing power. Pertinent thermodynamic and kinetic data featuring the oxidoreduction process are summarized in Table I.

Acknowledgment. This work was supported in part by the Centre national de la Recherche scientifique (Equipe de Recherche Associée 309 "Electrochimie Organique"). The Roussel-Uclaf Co. is gratefully thanked for the gift of B_{12a} samples.

References and Notes

- (1) (a) Laboratoire de Biophysique du Museum National d'Histoire Naturelle; (b) Laboratoire d'Electrochimie de l'Universit  de Paris VII.
- (2) J. M. Pratt, "Inorganic Chemistry of Vitamin B_{12} ", Academic Press, London and New York, 1972, pp 109-113, 151-152, 191-210.
- (3) J. M. Wood and D. G. Brown, *Struct. Bonding (Berlin)*, **11**, 47-105 (1972).
- (4) T. C. Stadtman, *Science*, **171**, 859-867 (1971).
- (5) H. Diehl, R. V. W. Haar, and R. R. Sealock, *J. Am. Chem. Soc.*, **72**, 5312-5313 (1950).
- (6) H. Diehl, J. I. Morrison, and R. R. Sealock, *Experientia*, **7**, 60 (1951).
- (7) R. N. Boos, J. E. Carr, and J. B. Conn, *Science*, **117**, 603-604 (1953).
- (8) B. Jaselskis and H. Diehl, *J. Am. Chem. Soc.*, **76**, 4345-4348 (1954).
- (9) D. Lexa and J. M. Lhoste, *Experientia, Suppl.*, **18**, 395-405 (1971).
- (10) B. A. Abd-El-Nabey, *J. Electroanal. Chem.*, **53**, 317-324 (1974).
- (11) T. H. Kenyhercz and H. B. Mark, *Anal. Lett.*, **7**, 1-7 (1974).
- (12) O. Muller and G. Muller, *Biochem. Z.*, **336**, 299-313 (1962).
- (13) H. P. C. Hogenkamp and S. Holmes, *Biochemistry*, **9**, 1886-1892 (1970).
- (14) K. Bernhauer, O. Muller, and F. Wagner, *Adv. Enzymol.*, **26**, 233-281 (1964).
- (15) B. Kratochvil and H. Diehl, *Talanta*, **13**, 1013-1017 (1966).
- (16) S. L. Tacket, J. W. Collat, and J. C. Abbott, *Biochemistry*, **2**, 919-923 (1963).
- (17) S. L. Tacket and J. W. Ide, *J. Electroanal. Chem.*, **30**, 510-514 (1971).
- (18) P. G. Swetik and D. G. Brown, *J. Electroanal. Chem.*, **51**, 433-439 (1974); *Biochem. Biophys. Acta*, **343**, 641-647 (1974).
- (19) R. L. Birke, G. A. Brydon, and M. F. Boyle, *J. Electroanal. Chem.*, **52**, 237-249 (1974).
- (20) H. A. O. Hill, J. M. Pratt, and R. P. J. Williams, *J. Chem. Soc.*, 5149-5154 (1964).
- (21) P. K. Das, H. A. O. Hill, J. M. Pratt, and R. P. J. Williams, *Biochem. Biophys. Acta*, **141**, 644-646 (1967).
- (22) P. K. Das, H. A. O. Hill, J. M. Pratt, and R. P. J. Williams, *J. Chem. Soc. A*, 1261-1264 (1968).
- (23) G. N. Schrauzer, E. Deutsch, and R. J. Windgassen, *J. Am. Chem. Soc.*, **90**, 2441-2442 (1968).
- (24) R. S. Firth, H. A. O. Hill, B. E. Mann, J. M. Pratt, and R. P. J. Williams, *Chem. Commun.*, 1013-1014 (1967).
- (25) D. Lexa and J. M. Sav ant, *Chem. Commun.*, 872-874 (1975).
- (26) G. Tortolani, P. Bianchini, and V. Mantovani, *Farmaco, Ed. Sci.*, **25**, 772-775 (1970).
- (27) J. A. Coch-Frugoni, *Gazz. Chim. Ital.*, **87**, 403-407 (1957).
- (28) D. Garreau and J. M. Sav ant, *J. Electroanal. Chem.*, **35**, 309-331 (1972).
- (29) H. Matsuda and Y. Ayabe, *Z. Electrochem.*, **59**, 494-503 (1955).
- (30) J. M. Sav ant, *Electrochim. Acta*, **12**, 999-1030 (1967).
- (31) J. Heyrovsky and J. Kuta, "Principles of Polarography", Academic Press, New York, N.Y., 1966, pp 287-295.
- (32) R. H. Wopshall and I. Shain, *Anal. Chem.*, **39**, 1514-1527 (1967).
- (33) J. M. Sav ant and E. Vianello, *Electrochim. Acta*, **8**, 905-923 (1963).
- (34) M. S. Shuman and I. Shain, *Anal. Chem.*, **41**, 1818-1825 (1969).
- (35) J. M. Sav ant and E. Vianello, *C. R. Hebd. Seances Acad. Sci.*, **256**, 2597-2600 (1963).
- (36) L. Nadjo and J. M. Sav ant, *J. Electroanal. Chem.*, **48**, 113-145 (1973).
- (37) J. W. Collat and J. C. Abbott, *J. Am. Chem. Soc.*, **86**, 2308-2309 (1964).
- (38) P. K. Das, *J. Chem. Soc., Dalton Trans.*, **23**, 2475-2479 (1974).
- (39) J. M. Sav ant and E. Vianello, "Advances in Polarography", Vol. 1, Langmuir, Ed., Pergamon Press, 1960, pp 367-374.
- (40) J. M. Sav ant and E. Vianello, *Electrochim. Acta*, **10**, 905-920 (1965).
- (41) D. S. Polcyn and I. Shain, *Anal. Chem.*, **38**, 376-382 (1966).